

光纤陀螺热致漂移分析及算法补偿技术研究

冷悦^{1,2,3*}, 钟胜^{1,2}¹华中科技大学人工智能与自动化学院, 湖北 武汉 430074;²多谱信息智能处理技术全国重点实验室, 湖北 武汉 430074;³华中光电技术研究所武汉光电国家研究中心, 湖北 武汉 430223

摘要 通过对光纤陀螺温度漂移的剖析推导,分析了温度扰动引起陀螺漂移误差的深层次原因,并结合过程相关性理论,对各个温度项影响因子与光纤陀螺实际输出相关性进行验证分析,提出一种同时考虑温度、温变速率、温度梯度以及三者乘积耦合项的算法补偿模型。对该模型的补偿效果进行离线补偿验证,结果表明,采用该算法补偿模型能明显抑制光纤陀螺的变温零漂。为了进一步验证该模型的有效性,把离线获得的补偿参数载入陀螺存储器,经过多样本实验测试,补偿后可有效提高光纤陀螺的全变温零偏稳定性,验证了该补偿算法在工程上的可实施性和推广价值。

关键词 光纤光学; 光纤陀螺; Shupe效应; 光纤环圈; 温变速率; 补偿算法

中图分类号 TH741

文献标志码 A

DOI: 10.3788/AOS231416

1 引言

偏光纤维技术、绕环工艺技术以及其他光器件技术的进步,使高精度光纤陀螺大批量应用于导航领域成为可能。但很多无人运载器平台对导航系统的尺寸、质量、功耗、成本控制等都有较高要求,因此通过加持温控系统来抑制光纤陀螺温度漂移问题不具有可操作性^[1]。光纤环圈是光纤陀螺的核心部件,但其制备过程仍然需要手工操作的介入,造成产品设计与制备成品存在差异,且外界温度扰动易造成性能恶化。虽然可以通过研制低温度敏感性光纤^[2-4]、改善绕制工艺及提高对称度^[5-9](例如,采用四极对称绕法、八极对称绕法乃至十六级对称绕制方法)、优化腔体结构设计^[10]、减缓温度扰动速率等手段加强陀螺自身的温漂自抑制能力,但一些人为因素、器件自身缺陷等造成陀螺温度性能下降仍无法有效解决^[11-14]。

依托光纤陀螺系统平台^[15],寻找陀螺输出与温度等相关因素的变化规律,通过算法补偿的手段可弱化光纤陀螺的热致误差影响。工程上通常依托多项式模型实施补偿^[16]。随着芯片运力的提升,依托模型驯化手段,近期一些智能算法补偿手段^[17-20]也备受研究者关注,但数据量巨大、光纤陀螺个体又存在差异性,补偿算法可移植性差,因此很难在工程上实际补偿应用。

本文从机理层面入手^[21],详细分析了光纤陀螺核心部件——光纤环圈受温度影响时所产生的相位误差导致陀螺性能变差的深层次原因,并对各温度因素的

影响情况进行了过程相关性分析,提出一种可工程化实现的新型多项式零漂温度补偿模型。基于该模型提出的补偿方案经过验证能明显抑制陀螺温度漂移误差。

2 理论基础

2.1 热致误差模型推导

光纤环自身温度场会受到周围温度扰动的影响,扰动作用到光纤环体后,会引起相应光纤段的折射率发生变化,而这种不对称的折射率变化无法有效抵消,最终会导致相移。这种因温度变化引起光纤折射率改变,进而导致陀螺输出出现漂移误差的情况被称为“纯”Shupe效应。

经过推导,热变化引起的漂移误差可表示为

$$\Omega_{E1}(t) = \frac{n}{DL} \cdot \left(\frac{\partial n}{\partial T} + n \cdot \alpha \right) \int_0^L \dot{T}(l, t) (L - 2l) dl, \quad (1)$$

式中: n 为光纤的有效折射率; D 为光纤环圈等效面积; dl 为光纤片段; α 为光纤的热膨胀系数; L 为光纤的长度。借助数学中 $\lim_{\Delta t \rightarrow 0} [f(t + \Delta t) - f(t)] / \Delta t = \dot{f}(t)$ 的微分定义,可得另一通用公式:

$$\Omega_{E1}(t) = \frac{n}{DL} \cdot \left(\frac{\partial n}{\partial T} + n \cdot \alpha \right) \int_0^{L/2} [\dot{T}(l, t) - \dot{T}(L - l, t)] (L - 2l) dl. \quad (2)$$

由式(1)可知,光纤干涉仪的漂移误差与光纤环圈各个光纤片段温度场的变化率 $\dot{T}(l, t)$ 也有关,因此通

过优化结构设计、减缓温度场变化可有效降低由热引起的漂移误差,由式(2)可知, $\dot{T}(l, t) - \dot{T}(L - l, t)$ 越小,热致漂移误差越小,因此光纤环圈中点两侧的热场对称性越高,则抑制热致温度漂移误差的效果越好。

在变温条件下,光纤环圈中各光纤片段会进行热胀冷缩,而光纤环圈中胶黏剂、涂覆层、纤芯会相互挤压,从而引起折射率变化。经过推导,热应力引起的两个等价漂移误差^[15]可以表示为

$$\Omega_{E2}(t) = \frac{n}{DL} \left\{ \frac{2\nu n}{E} + \frac{n^3}{2E} [P_{11}(1-\nu) + P_{12}(1-3\nu)] \right\} \int_0^L \dot{P}(l, t)(L-2l)dl, \quad (3)$$

$$\Omega_{E2}(t) = \frac{n}{DL} \left\{ \frac{2\nu n}{E} + \frac{n^3}{2E} [P_{11}(1-\nu) + P_{12}(1-3\nu)] \right\} \int_0^{L/2} [\dot{P}(l, t) - \dot{P}(L-l, t)](L-2l)dl, \quad (4)$$

式中: P_{11} 、 P_{12} 为光纤材料的弹光系数; E 为弹性模量系数; ν 为泊松比系数。由式(3)可知,热应力引起的漂移误差与光纤自身温度有关;由式(4)可知,热应力引起的漂移误差与光纤片段所处位置也有关。光纤环圈中点两侧相对应的光纤片段处于不同的层位置和匝位置,其所受相邻光纤的挤压不同。即使光纤环圈温度趋于恒定,应力引起的折射率变化也无法完全抵消,在变温情况下,应力引起的折射率变化更为复杂。因此,“纯”Shupe 效应无法全面表征温度变化引起的漂移误差,热应力误差因素是不可忽略的。

综上,光纤陀螺总的热致误差漂移公式为

$$\Omega_E(t) = \Omega_{E1}(t) + \Omega_{E2}(t). \quad (5)$$

2.2 建模补偿

由上述分析可知,温度变化引起的光纤陀螺漂移误差与温度变化引起的光纤折射率变化、热应力变化引起的光纤折射率变化、温度变化引起的折射率变化速率、热应力变化引起的折射率变化速率、光纤环圈中点两侧光纤各片段空间层面热场分布对称情况、光纤环圈中点两侧光纤各片段空间层面热应力分布对称情况等因素有关。设计时,热场均化设计、微应力光纤黏接工艺、光纤环圈多极对称绕制工艺等的引入,虽然可最大限度弱化温度扰动引起的偏差,但是无法完全消除,因此只有通过寻找陀螺输出与温度相关因素的关联性,通过补偿的手段进一步提升陀螺性能。光纤陀螺温度补偿的效果与所建立模型的准确度直接相关,即通过实验手段寻找陀螺输出数据与对应激励温度的关系,并进行准确辨识,然后根据建成的模型设计相应的算法进行补偿。

光纤陀螺零偏温度漂移的建模,就是寻找陀螺输出结果与温度扰动因素的内在关系。依据 IEEE 给出的定义,光纤陀螺的热致误差模型可以表述为

$$f = L - L_0 = \sum_{i=1}^{\alpha} A_i (T - T_0)^i + \sum_{j=1}^{\beta} B_j \left(\frac{dT}{dt} \right)^j + \sum_{k=1}^p C_k (T - T_{ave})^k \quad (6)$$

式中: f 为热致误差; L 为陀螺输出; L_0 为陀螺输出均值; T 为环圈实时温度; T_0 为环圈起始温度; T_{ave} 为环圈内外壁均值温度; dT/dt 为环圈温变速率; α 、 A_i 分别为温度因素的最高次幂和对应系数; β 、 B_j 分别为温变速率因素的最高次幂和对应系数; p 、 C_k 分别为温度梯度因素的最高次幂和对应系数。

运用回归分析最小二乘法对模型多项式中的系数 A_i 、 B_j 、 C_k 进行拟合计算。多项式模型可表示为

$$L - L_0 = Ta, \quad (7)$$

$$\text{式中: } T = \begin{bmatrix} T_1 & T_1^2 & \cdots & T_1^q \\ T_2 & T_2^2 & \cdots & T_2^q \\ \vdots & \vdots & \ddots & \vdots \\ T_N & T_N^2 & \cdots & T_N^q \end{bmatrix}; \quad a = \begin{bmatrix} a_1 \\ a_2 \\ \vdots \\ a_q \end{bmatrix}; \quad a_\xi (\xi =$$

1, 2, ..., q) 为温度项系数; q 为模型阶数; $T_\xi (\xi = 1, 2, \dots, N)$ 为光纤环圈的实时温度; T_ξ^q 为温度因素; N 为温漂数据的个数。

不同温度下拟合的系数是不同的,式(6)中 A_i 、 B_j 、 C_k 满足如下关系:

$$\begin{cases} a_1 = A_{10} + A_{11}T_0 + A_{12}T_0^2 + A_{13}T_0^3 \\ a_2 = A_{20} + A_{21}T_0 + A_{22}T_0^2 + A_{23}T_0^3 \\ \vdots \\ a_q = A_{q0} + A_{q1}T_0 + A_{q2}T_0^2 + A_{q3}T_0^3 \end{cases}. \quad (8)$$

在实际使用中,对不同温度下的陀螺通过最小二乘法进行计算,可得到系数 $A_{\xi\eta} (\xi=1, 2, \dots, q; \eta=0, 1, 2, 3)$ 。将其烧写进陀螺处理单元存储芯片中,只要在陀螺启动后通过温度传感器探测到初始温度 T_0 ,即可根据式(8)算出系数值。然后,依据式(6)考虑各温度因素,估计出陀螺实际热致零偏,并将该估计零偏扣除,即为补偿后的零偏。

为了进一步剖析各温度影响因子与光纤陀螺输出的相关性,依据式(9),通过仿真分析手段进行对比分析。

$$r = \frac{\sum_{i=1}^{\alpha} (x_i - \bar{x})(y_i - \bar{y})}{\sqrt{\sum_{i=1}^{\alpha} (x_i - \bar{x})^2 \cdot \sum_{i=1}^{\alpha} (y_i - \bar{y})^2}} = \frac{\alpha \sum_{i=1}^{\alpha} x_i y_i - \sum_{i=1}^{\alpha} x_i \cdot \sum_{i=1}^{\alpha} y_i}{\sqrt{\alpha \sum_{i=1}^{\alpha} x_i^2 - \left(\sum_{i=1}^{\alpha} x_i \right)^2} \cdot \sqrt{\alpha \sum_{i=1}^{\alpha} y_i^2 - \left(\sum_{i=1}^{\alpha} y_i \right)^2}}, \quad (9)$$

式中: r 为相关系数; x 为影响因素(温度、温度变化率等); y 为陀螺输出。根据式(9)可分析光纤陀螺输出

与各温度因素的过程相关性,进而完善补偿模型。

3 实验与分析

3.1 补偿算法验证与分析

将某 120 型单轴光纤陀螺放置在隔振温箱内(名称:温控转台;设备型号:HEOS/WKZT1-40B),实验环境如图 1 所示。

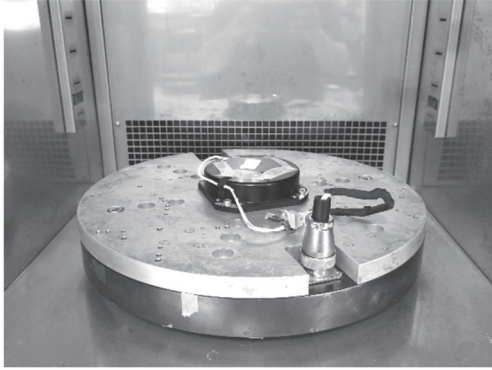


图 1 测试现场图
Fig. 1 Test field diagram

控制温箱在 25 °C 保温 1 h,之后以 1 °C/min 的温变速率将温箱内的温度降低到 -40 °C,保温 2 h;以 1 °C/min 的温变速率将温箱内温度升温至 65 °C,保温 2 h;控制温箱将温箱内温度以 1 °C/min 降低至 25 °C,温箱停止工作。陀螺输出及温度输出曲线如图 2 所示。经过统计计算,陀螺补偿前零偏值为 7.631 (°)/h,零偏稳定性(100 s 平滑)为 0.0516 (°)/h。

传统情况下,光纤陀螺内部只放置一个温度传感器,只能获得光纤环圈体表面的温度、温变速率两项因素,无法表征温度梯度影响因素。只考虑温度和温变速率两项因素,依据相关性理论,绘制出陀螺输出与温度和温变速率的过程相关曲线。

由图 3 可知:整个变温过程中,陀螺输出与温变速率过程相关度很高(红色虚线),相关度高于 0.8;陀螺输出与温度的过程相关度(蓝实线)在变温起始到恒温保持过程中呈现负相关,相关度低于 -0.8,而在低温

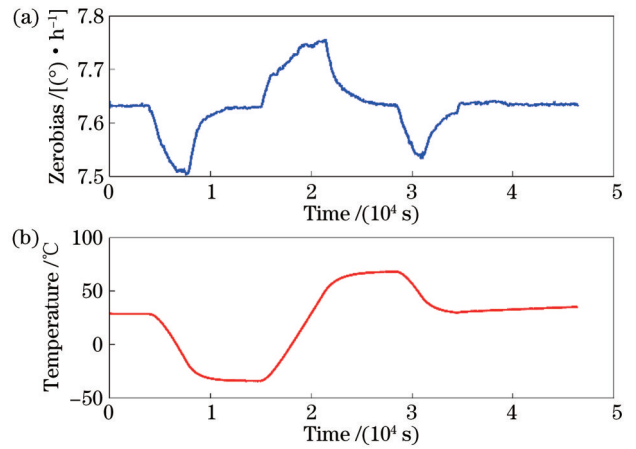


图 2 陀螺输出及温度曲线。(a)零偏曲线;(b)温度曲线
Fig. 2 Gyroscope output and temperature curves. (a) Zerobias curve; (b) temperature curve

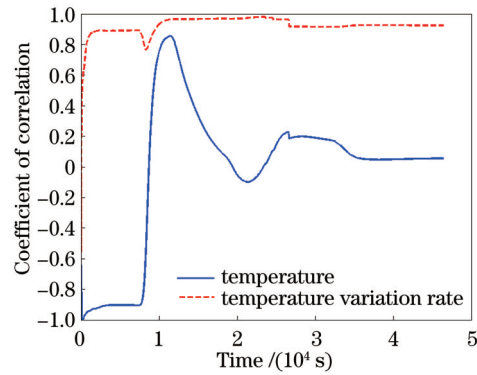


图 3 变温过程相关曲线

Fig. 3 Temperature change process correlation curve

保持过程中呈现正相关,之后都处于较低水平。因此,在整个变温过程中,需要综合考虑此两项温度项因素进行补偿。

由表 1 可知,只考虑温度、温变速率两项因素,一阶情况下,变温零偏稳定性已达最优效果,达到 0.0059 (°)/h,而二阶补偿效果与一阶补偿效果相同。模型阶数越高,计算量越大,考虑到光纤陀螺存在差异性,为确保补偿效果,温度和温变速率都定为二阶。

表 1 考虑温度、温变速率因素的不同阶补偿效果

Table 1 Different compensation effects of temperature and temperature variation rate factors

Item	Temperature	Temperature variation rate	Zero offset / [(°)·h ⁻¹]	Variable temperature zerobias stability (100 s smoothing) / [(°)·h ⁻¹]
1	Zero-order	Zero-order	7.631	0.0516
2	First-order	Zero-order	7.631	0.0514
3	Zero-order	First-order	7.631	0.0069
4	First-order	First-order	7.631	0.0059
5	Second-order	First-order	7.631	0.0059
6	First-order	Second-order	7.631	0.0059
7	Second-order	Second-order	7.631	0.0059

综合考虑陀螺输出零偏与温度、温变速率的关系,建立光纤陀螺温度补偿模型为二阶温度补偿模型,具体为

$$E = A_1 \cdot (T - T_0) + B_1 \cdot \frac{dT}{dt} + A_2 \cdot (T - T_0)^2 + B_2 \cdot \left(\frac{dT}{dt}\right)^2 \quad (10)$$

依据第 2 节的热致误差机理分析,以及光纤陀螺的实际装配体情况,光纤陀螺环体温度影响因素是复杂的,尤其是在光纤陀螺变温过程中,由于光纤环圈自身安装形式及结构特性,不同位置的热场必然存在差异性,启动后会有热传导,存在梯度变化情况。温度、温变速率这两项补偿因素在补偿趋势方面具有很好的效果,但是无法反映环体自身热传导过程,因此综合考虑单轴光纤陀螺自身的结构特点,除在环体上部加装一个温度传感器 TS₁ 外,在干涉仪模块磁屏蔽靠近底部位置再加装一个数字温度传感器 TS₂,综合实时反映光纤环圈体动态温度趋势。两个温度传感器的位置如图 4 所示。温箱变温过程中,陀螺内两个温度传感器 TS₁ 和 TS₂ 的温度曲线如图 5 所示。

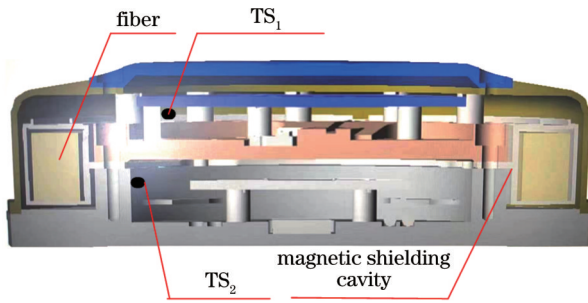


图 4 两个温度传感器的分布位置图
Fig. 4 Location diagram of two temperature sensors

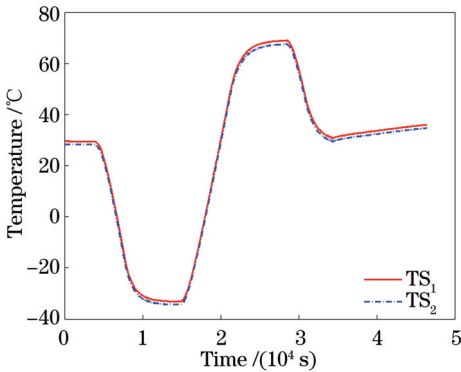


图 5 两个温度传感器的输出曲线
Fig. 5 Output curves of two temperature sensors

温度、温变速率、温度梯度的相关性分析结果如图 6 线所示。陀螺输出与温度梯度的相关性在变温过程中都有体现,因此不可忽略。直接考虑二阶因素影响,则补偿模型可完善为

$$E = A_1 \cdot (T - T_0) + B_1 \cdot \frac{dT}{dt} + C_1 \cdot (T - T_{ave}) + A_2 \cdot (T - T_0)^2 + B_2 \cdot \left(\frac{dT}{dt}\right)^2 + C_2 \cdot (T - T_{ave})^2 \quad (11)$$

式中: T_{ave} 为陀螺中两个温度传感器采集数据的均值。

$$T_{ave} = \frac{T_{s1} + T_{s2}}{2} \quad (12)$$

式中: T_{s1} 和 T_{s2} 分别为温度传感器 TS₁ 和 TS₂ 采集的温度。

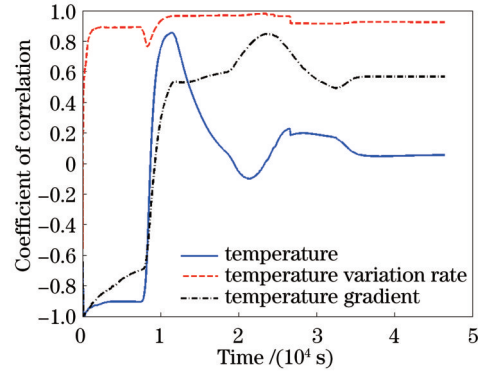


图 6 考虑温度、温变速率、温度梯度的过程相关性
Fig. 6 Process correlation considering temperature, temperature variation rate, and temperature gradient

从图 7 可以看到:补偿前,光纤陀螺变温零偏稳定性(100 s 平滑)为 0.0516 (°)/h;不考虑温度梯度因素,只考虑温度和温变速率因素,补偿后陀螺变温零偏稳定性(100 s 平滑)为 0.0059 (°)/h;如果同时考虑温度、温变速率、温度梯度三项因素,补偿后光纤陀螺输出零偏为 7.631 (°)/h,变温零偏稳定性(100 s 平滑)可达 0.0050 (°)/h,补偿效果提升 15% 左右。因此,通过添加两个温度传感器进行光纤陀螺温度补偿是一种可实时且有效地抑制温度漂移的方法。

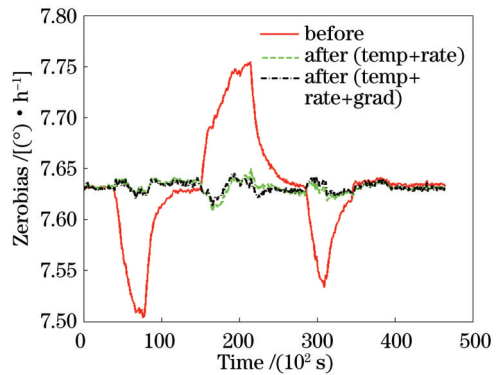


图 7 补偿前后陀螺输出对比曲线
Fig. 7 Gyroscope output contrast curves before and after compensation

3.2 补偿算法优化与验证

由式(3)和式(4)可知,温度对光纤环圈环体的影响是复杂的,温度偏离固有温度点后,光纤中的石英纤

芯、涂覆层、胶黏剂因膨胀系数不同,热胀冷缩时会存在相互挤压现象,这种挤压会造成空间应力变化,而这种变化无法通过传统 Shupe 误差模型进行评估,只能通过一些与温度相关的耦合因素项进行表征。因此,存在温度、温变速率、温度梯度三项温度因素无法表征的影响因素,将其定义为乘积耦合项,即温度、温变速率、温度梯度三者的乘积。通过过程相关性分析,在变温阶段乘积耦合项与陀螺输出也存在较高的相关度,因此该影响因素不可忽略,如图 8 所示。

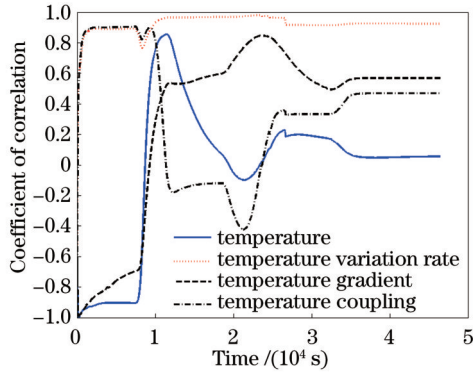


图 8 考虑耦合项因素的过程相关性曲线

Fig. 8 Process correlation curves considering coupling term factors

根据过程相关性分析,温度补偿模型可进一步完善为

$$E = A_1 \cdot (T - T_0) + B_1 \cdot \frac{dT}{dt} + C_1 \cdot (T - T_{ave}) + D_1 \cdot (T - T_0) \cdot \frac{dT}{dt} \cdot (T - T_{ave}) + A_2 \cdot (T - T_0)^2 + B_2 \cdot \left(\frac{dT}{dt}\right)^2 + C_2 \cdot (T - T_{ave})^2 + D_2 \cdot \left[(T - T_0) \cdot \frac{dT}{dt} \cdot (T - T_{ave}) \right]^2, \quad (13)$$

式中: D_1 为温度、温变速率和温度梯度乘积耦合项的一阶系数; D_2 为温度、温变速率和温度梯度乘积耦合项的二阶系数。

基于所提算法补偿模型进行离线补偿验证,光纤陀螺输出零偏为 $7.631 (^{\circ})/h$,变温零偏稳定性(100 s 平滑) $0.0037 (^{\circ})/h$,补偿效果明显(图 9)。

为了进一步对上述理论模型和算法进行验证,除保留仿真验证的首个样本外(命名为 001 号),同时新增加 2 个样本(依次命名为 002 号、003 号)进行 $-40 \sim 65 ^{\circ}C$ 的全变温补偿实验验证,补偿前 3 个样本的变温测试对比曲线如图 10 所示。补偿前变温情况下 001 号、002 号、003 号样本的零偏稳定性依次分别为 $0.050 (^{\circ})/h$ 、 $0.006 (^{\circ})/h$ 、 $0.01 (^{\circ})/h$ 。

将补偿后 3 个陀螺样品安装在高精度温箱内,温箱温度变化程序设定为 $(25 ^{\circ}C, 120 \text{ min}) \rightarrow (-40 ^{\circ}C,$

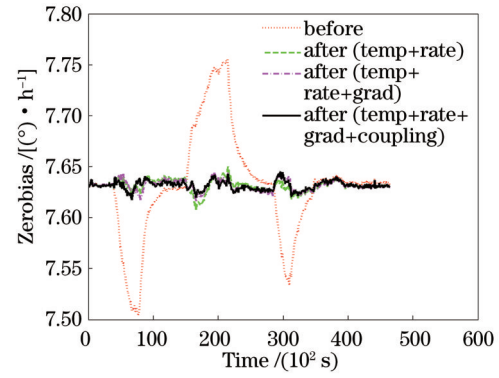


图 9 考虑耦合项因素的算法补偿效果

Fig. 9 Algorithm compensation effect considering coupling term factor

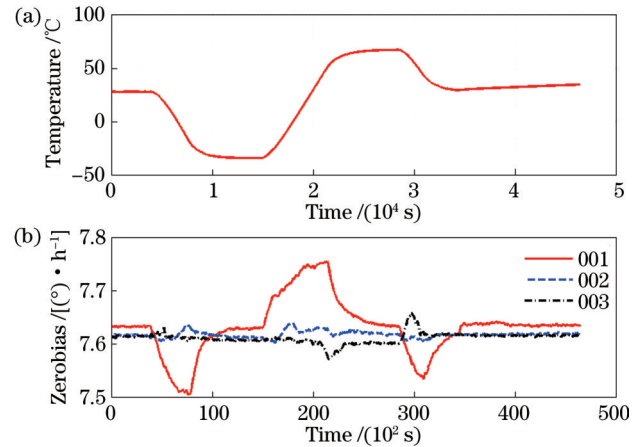


图 10 算法补偿前陀螺实验测试结果。(a)温度曲线;(b)零偏曲线

Fig. 10 Results of gyroscope experiment before algorithm compensation. (a) Temperature curve; (b) zerobias curves

$120 \text{ min}) \rightarrow (65 ^{\circ}C, 120 \text{ min}) \rightarrow (25 ^{\circ}C, 120 \text{ min})$,升降温过程中温箱温变速率设置为 $1 ^{\circ}C/\text{min}$,在 25 、 -40 、 $65 ^{\circ}C$ 的恒温时间均设置为 120 min ,以验证补偿效果。实时同步记录光纤陀螺内的输出和温度数据,并对输出数据进行 100 s 平滑,测试曲线如图 11 所示,补偿后的 001 号、002 号、003 号样本的零偏稳定性分别为 $0.0036 (^{\circ})/h$ 、 $0.004 (^{\circ})/h$ 、 $0.0041 (^{\circ})/h$ 。

经统计,补偿后陀螺零偏稳定性(100 s 平滑)的实测精度均提高,证明了考虑耦合项影响因素的温度补偿模型算法的有效性。

4 结 论

结合热致误差机理推导分析及过程相关性理论,对光纤陀螺温度补偿算法模型进行剖析,提出一种同时考虑温度、温变速率、温度梯度及三者乘积耦合项的新型多项算法补偿模型。通过离线补偿手段,验证了所提算法的可行性,补偿后陀螺零偏稳定性精度与只考虑温度、温变速率、温度梯度这三项因素的补偿算法相比,补偿效果提升明显。另外,通过多样本实验的手

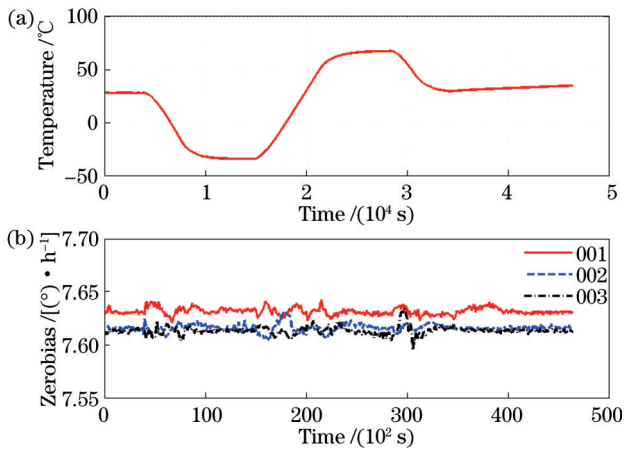


图 11 算法补偿后陀螺实验测试结果。(a)温度曲线;(b)零偏曲线

Fig. 11 Results of gyroscope experiment after algorithm compensation. (a) Temperature curve; (b) zerobias curves

段将补偿参数烧入陀螺中,在变温($-40\sim 65\text{ }^{\circ}\text{C}$, $1\text{ }^{\circ}\text{C}/\text{min}$)条件下进行全变温实验验证。实验结果表明,在变温条件下,3个光纤陀螺样本的零偏稳定性均优于 $0.005\text{ }(^{\circ})/\text{h}$ (100 s 平滑),补偿效果达到预期效果。由于光纤陀螺各个单体存在差异性,下一步将通过大批量实验来验证算法的有效性。

参 考 文 献

- 范运强,黄继勋,李晶.基于局部光路温度控制的光纤陀螺温度误差抑制方法[J].中国惯性技术学报,2020,28(6):809-813.
Fan Y Q, Huang J X, Li J. Fiber optic gyroscope temperature error suppression method with local optical path temperature control[J]. Journal of Chinese Inertial Technology, 2020, 28(6): 809-813.
- 毕聪志,杨纪刚,吴衍记,等.光纤陀螺用保偏光纤温度敏感性测试与分析[J].中国惯性技术学报,2014,22(5):677-681.
Bi C Z, Yang J G, Wu Y J, et al. Temperature sensitivity measurement and analysis of polarization maintaining fiber for FOG[J]. Journal of Chinese Inertial Technology, 2014, 22(5): 677-681.
- 杨博,滕飞,张智昊,等.高精度光子晶体光纤陀螺设计及在轨应用验证[J].中国惯性技术学报,2022,30(1):113-120.
Yang B, Teng F, Zhang Z H, et al. On orbit validation and design of high precision photonic crystal fiber optic gyroscope[J]. Journal of Chinese Inertial Technology, 2022, 30(1): 113-120.
- 张春熹,张祖琛,高福宇.光子晶体光纤陀螺技术[J].光学学报,2022,42(17):1706002.
Zhang C X, Zhang Z C, Gao F Y. Photonic crystal fiber optic gyro technology[J]. Acta Optica Sinica, 2022, 42(17): 1706002.
- 王玥泽,陈晓冬,张桂才,等.八极绕法对光纤陀螺温度性能的影响[J].中国惯性技术学报,2012,20(5):617-620.
Wang Y Z, Chen X D, Zhang G C, et al. Effect of octupole-winding on temperature performance of fiber optic gyroscope[J]. Journal of Chinese Inertial Technology, 2012, 20(5): 617-620.
- 李绪友,张春梅,刘华兵,等.光纤环十六极对称绕法温度性能的仿真与分析[J].中国惯性技术学报,2016,24(6):780-785.
Li X Y, Zhang C M, Liu H B, et al. Simulation and analysis on temperature performance of fiber ring by 16-polar symmetrical winding method[J]. Journal of Chinese Inertial Technology, 2016, 24(6): 780-785.
- 范运强,黄继勋,李晶.干涉光路装配应力对称性对 Shupe 误差的影响[J].光学学报,2021,41(21):2112002.
Fan Y Q, Huang J X, Li J. Effect of assembly stress symmetry of interference optical path on Shupe error[J]. Acta Optica Sinica, 2021, 41(21): 2112002.
- 范运强,黄继勋,李晶.基于等效不对称长度的光纤环温度性能评价方法[J].光学学报,2021,41(23):2306002.
Fan Y Q, Huang J X, Li J. Temperature performance evaluation of fiber coil with equivalent asymmetric length[J]. Acta Optica Sinica, 2021, 41(23): 2306002.
- 李绪友,凌卫伟,许振龙,等.双柱型绕法对干涉式光纤陀螺温度性能的影响[J].光学学报,2016,36(8):0806003.
Li X Y, Ling W W, Xu Z L, et al. Effect of double-cylinder winding on temperature performance of interferometric fiber optic gyroscope[J]. Acta Optica Sinica, 2016, 36(8): 0806003.
- 李绪友,凌卫伟,许振龙,等.基于交叉法绕制的光纤环的槽体设计[J].光学学报,2015,35(6):0606002.
Li X Y, Ling W W, Xu Z L, et al. Design of a new spool for fiber coil based on cross winding pattern[J]. Acta Optica Sinica, 2015, 35(6): 0606002.
- 闫晗,杨远洪,杨福铃.光纤陀螺热扩散延迟响应模型及补偿技术研究[J].中国激光,2019,46(1):0106003.
Yan H, Yang Y H, Yang F L. Response model and compensation technology of thermal diffusion delay in fiber optic gyro coil[J]. Chinese Journal of Lasers, 2019, 46(1): 0106003.
- Shupe D M. Thermally induced nonreciprocity in the fiber-optic interferometer[J]. Applied Optics, 1980, 19(5): 654-655.
- 邱嘉华,王磊,黄腾超,等.干涉式光纤陀螺技术发展综述[J].光学学报,2022,42(17):1706004.
Qiu J L, Wang L, Huang T C, et al. Review of development of interferometric fiber optic gyroscope technology development[J]. Acta Optica Sinica, 2022, 42(17): 1706004.
- Mohr F. Thermo-optically induced bias drift in fiber optical Sagnac interferometers[J]. Journal of Lightwave Technology, 1996, 14(1): 27-41.
- 凌卫伟.光纤陀螺温度效应机理分析及补偿措施研究[D].哈尔滨:哈尔滨工程大学,2017:1-10.
Ling W W. Mechanism analysis of temperature effect of fiber optic gyro and research on compensation measures[D]. Harbin: Harbin Engineering University, 2017: 1-10.
- 孙英杰.光纤陀螺温度漂移误差建模及补偿技术研究[D].哈尔滨:哈尔滨工业大学,2010:14-28.
Sun Y J. Research on modeling and compensation technology of temperature drift error of fiber optic gyroscope[D]. Harbin: Harbin Institute of Technology, 2010: 14-28.
- 延凤平,蓝慧娟,简水生.光纤陀螺温度补偿方案研究[J].光学学报,1999,19(7):968-974.
Yan F P, Lan H J, Jian S S. Investigation of the temperature compensated method for fiber optic gyros[J]. Acta Optica Sinica, 1999, 19(7): 968-974.
- 李家垒,许化龙,何婧.基于小波网络的光纤陀螺启动漂移温度补偿[J].光学学报,2011,31(5):0506005.
Li J L, Xu H L, He J. Temperature compensation of start-up drift for fiber optic gyroscope based on wavelet network[J]. Acta Optica Sinica, 2011, 31(5): 0506005.
- 毛宁,许江宁,何泓洋,等.基于 Online-SVR 模型的光纤陀螺零漂实时补偿[J].激光与光电子学进展,2022,59(1):0106002.
Mao N, Xu J N, He H Y, et al. Real-time compensation of fiber optic gyroscope zero-drift based on online-SVR model[J]. Laser & Optoelectronics Progress, 2022, 59(1): 0106002.
- 刘元元,杨功流,李思宜. BP-AdaBoost 模型在光纤陀螺零偏温度补偿中的应用[J].北京航空航天大学学报,2014,40(2):235-239.
Liu Y Y, Yang G L, Li S Y. Application of BP-AdaBoost model in temperature compensation for fiber optic gyroscope bias [J]. Journal of Beijing University of Aeronautics and Astronautics, 2014, 40(2): 235-239.
- Zhang Y G, Gao Z X, Wang G C, et al. Modeling of thermal-

Thermal-Induced Drift Analysis and Algorithm Compensation Technology of Fiber Optic Gyroscope

Leng Yue^{1,2,3*}, Zhong Sheng^{1,2}

¹*School of Artificial Intelligence and Automation, Huazhong University of Science and Technology, Wuhan 430074, Hubei, China;*

²*National Key Laboratory of Multispectral Information Intelligent Processing Technology, Wuhan 430074, Hubei, China;*

³*Wuhan National Laboratory for Optoelectronics, Huazhong Institute of Electro-Optics, Wuhan 430223, Hubei, China*

Abstract

Objective Due to the advances in polarization-maintaining fiber technology, coil-winding process technology, and other optical fiber device technologies, high-precision fiber optic gyroscopes have been made possible for high-volume applications in navigation. However, in many unmanned vehicle platforms, the size, weight, power consumption, and cost control of the navigation system have high requirements, so it is not operable to suppress the temperature drift problem of fiber optic gyroscopes by adding a temperature control system. The fiber optic coil is the core component of the fiber optic gyroscope, but its preparation process requires the intervention of manual operation, resulting in a difference and poor consistency in product design and finished product, and its performance will deteriorate due to the external temperature perturbation. Although the development of low-temperature-sensitive optical fiber can improve the winding process to improve symmetry, optimize the cavity structure design, and slow down the rate of temperature perturbation to strengthen the gyroscope's self-suppressing ability of temperature drift, the gyroscope's temperature performance degradation caused by some human factors, device defects, and other factors is still unable to be effectively solved. Based on this, by relying on the fiber optic gyroscope system platform, we find the relationship between gyroscope output and temperature and other related factors and use algorithmic compensation to weaken thermally induced error effects of fiber optic gyroscopes. In this thesis, we start from the mechanism level and discuss and deduce in detail the deep-seated reasons for the deterioration of gyroscope performance due to the phase error caused by the temperature influence of the fiber optic coil, which is the core component of the fiber optic gyroscope, and we carry out the process correlation analysis of the influence of the temperature factors and put forward a new type of zero-drift polynomial temperature compensation model that can be realized in an engineered way. The proposed compensation scheme based on this model is verified to be effective and can significantly suppress the gyroscope temperature drift error.

Methods Through the fiber optic gyroscope temperature drift profiling derivation, the deep-seated causes of gyroscope drift error caused by temperature perturbation are analyzed, and the correlation of each temperature term influence factor with the actual output of fiber optic gyroscope is verified by combining with the process correlation theory. It is found that a temperature sensor can only characterize two temperature factors, temperature and temperature variation rate, but not the temperature gradient factor. Simulation analysis based on the process correlation theory shows that the compensation effect can be improved by introducing the temperature gradient factor under variable temperature conditions. In view of the fiber material properties, when the temperature changes, it will cause the material properties to change. Through simulation analysis, it is found that the output of the fiber optic gyroscope is correlated with the coupling factors of the product of temperature, temperature variation rate, and temperature gradient under variable temperatures. Finally, based on the relevant theoretical analysis, a temperature compensation algorithm model is established by simultaneously considering the temperature, temperature variation rate, temperature gradient, and the product of the three factors, and the validity of the model is verified through experiments.

Results and Discussions Through theoretical analysis, it is found that the fiber optic gyroscope cannot characterize the temperature gradient factor with the help of only one temperature sensor. Therefore, an implementation method of adding two temperature sensors inside the fiber optic gyroscope is proposed (Fig. 4). Simulation analysis with the help of process correlation theory (Fig. 6) reveals that there is indeed a correlation between the output of the fiber optic gyroscope and the temperature gradient factor during the temperature change process, which further supports the accuracy of the

aforementioned theoretical analysis. Therefore, the temperature gradient factor is introduced when the compensation model is established. Through the offline comparison simulation test, it is concluded that the compensation model considering the temperature gradient factor can further improve the accuracy of the compensation model and enhance the gyroscope temperature performance (Fig. 7). In addition, by further analyzing the mechanism of thermally induced error in fiber optic gyroscope and verifying it with the help of process correlation theory simulation, a more comprehensive compensation model (Eq. 12) is proposed by simultaneously considering the temperature factor, the temperature variation rate factor, the temperature gradient factor, and the coupling term of the product of the three factors. Finally, the new temperature compensation model is verified to be more accurate and better compensated by means of multi-sample experiments (Fig. 11).

Conclusions In this paper, a new multinomial algorithm compensation model is proposed, which simultaneously considers the temperature factor, the temperature variation rate factor, the temperature gradient factor, and the coupling term of the product of the three factors. We combine the analysis of thermally induced error mechanism derivation and process correlation theory as the designation idea and analyze the temperature compensation algorithm model of fiber optic gyroscopes. The feasibility of the algorithm is verified through offline compensation, and the zero-bias stability accuracy of the gyroscope after compensation is significantly improved compared with the compensation algorithm that only considers three factors, namely, temperature factor, temperature variation rate, and temperature gradient. In addition, the compensation parameters are burned into the gyroscope by means of multi-sample experiments, and the full variable temperature experiments are carried out under variable temperature conditions ($-40-65\text{ }^{\circ}\text{C}$, $1\text{ }^{\circ}\text{C}/\text{min}$) for verification. The experimental results show that under the variable temperature conditions, the zero-bias stability of the three fiber optic gyroscope samples is better than $0.005\text{ }(^{\circ})/\text{h}$ (100 s smoothing), and the compensation effect reaches the expected effect. Due to the variability of the fiber optic gyroscope, the next step is to verify the effectiveness of the algorithm through large-volume experiments.

Key words fiber optics; fiber optic gyroscope; Shupe effect; fiber coil; temperature variation rate; compensation algorithm